2014

Enhanced Broadband Parametric Wavelength Conversion in Silicon Waveguide With the Multi-Period Grating

Xianting Zhang
Beijing University of Posts and Telecommunications

Jinhui Yuan
Beijing University of Posts and Telecommunications

Jiaziu Zou
Beijing University of Posts and Telecommunications

See next page for additional authors

Recommended Citation

X. Zhang et al. (2014). Enhanced broadband parametric wavelength conversion in silicon waveguide with the multi-period grating. *"EEE Photonics Journal*, vol. 6 (6), pp. 1-14. doi: 10.1109/JPHOT.2014.2366150

IEEE Photonics Journal
An IEEE Photonics Society Publication

Open Access

Enhanced Broadband Parametric Wavelength Conversion in Silicon Waveguide With the Multi-Period Grating

Volume 6, Number 6, December 2014

Xianting Zhang
Jinhui Yuan
Jiaxiu Zou
Boyuan Jin
Xinzhu Sang
Qiang Wu
Chongxiu Yu
Gerald Farrell

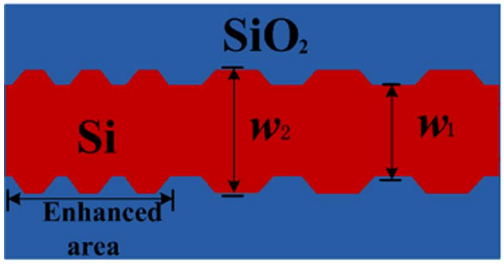

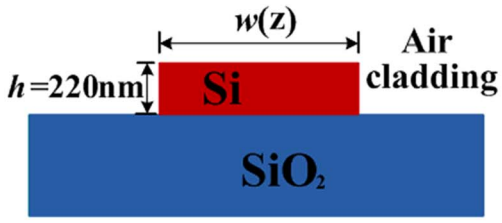

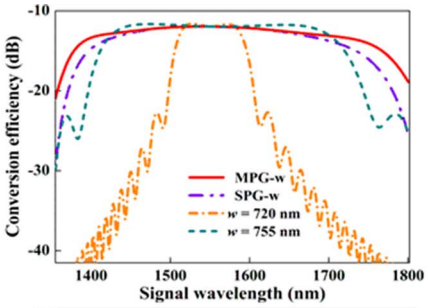

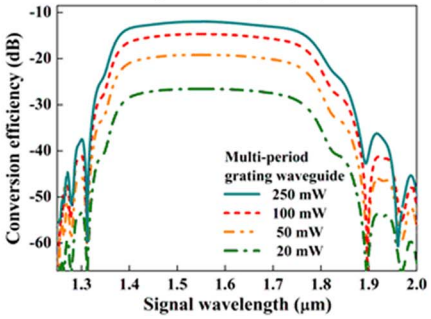

DOI: 10.1109/JPHOT.2014.2366150
1943-0655

IEEE photonics SOCIETY

IEEE

Enhanced Broadband Parametric Wavelength Conversion in Silicon Waveguide With the Multi-Period Grating

Xianting Zhang,[1] Jinhui Yuan,[1,3] Jiaxiu Zou,[2] Boyuan Jin,[1] Xinzhu Sang,[1] Qiang Wu,[1,4] Chongxiu Yu,[1] and Gerald Farrell[4]

[1]State Key Laboratory of Information Photonics and Optical Communications, Beijing University of Posts and Telecommunications, Beijing 100876, China
[2]School of Electronic Engineering, Beijing University of Posts and Telecommunications, Beijing 100876, China
[3]Photonics Research Center, Department of Electronic and Information Engineering, The Hong Kong Polytechnic University, Kowloon, Hong Kong
[4]Photonics Research Center, School of Electronic and Communications Engineering, Dublin Institute of Technology, Dublin 8, Ireland

DOI: 10.1109/JPHOT.2014.2366150

Manuscript received September 4, 2014; revised October 14, 2014; accepted October 14, 2014. Date of publication November 3, 2014; date of current version November 19, 2014. This work was supported in part by the National Basic Research Program under Grant 2010CB327601; by the National Natural Science Foundation of China under Grant 61307109, Grant 61475023, and Grant 61475131; by the Hong Kong Scholars Program 2013 under Grant PolyU G-YZ45; by the Program for New Century Excellent Talents in University under Grant NECT-11-0596 and Beijing Nova Program under Grant 2011066; by the National High-Technology Research and Development Program of China under Grant 2013AA031501; by the Specialized Research Fund for the Doctoral Program of Higher Education under Grant 20120005120021; by the Fundamental Research Funds for the Central Universities under Grant 2013RC1202; by the Fund of State Key Laboratory of Information Photonics and Optical Communications (Beijing University of Posts and Telecommunications), P. R. China; and by the Science Foundation Ireland (SFI) under Grant SFI/12/ISCA/2496 and Grant SFI/13/ISCA/2845. Corresponding author: J. Yuan (e-mail: yuanjinhui81@163.com).

Abstract: In this paper, a novel silicon-on-insulator (SOI) waveguide with the multi-period vertical grating is proposed to realize broadband parametric wavelength conversion with a quasi-phase matching technique. The grating period in the former part of the SOI waveguide is optimized to enhance the conversion efficiency at designated signal wavelength and the 3-dB bandwidth. When the continuous-wave pump at 1550 nm is used, the conversion efficiency of −14.0 dB at 1750 nm and the 3-dB bandwidth of 387 nm can be obtained. Compared to the constant-width waveguide, the improvements of 26.7 dB and 298 nm are achieved, respectively. The results show that this SOI waveguide is an ideal device for broadband wavelength conversion without dispersion engineering.

Index Terms: Multi-period grating, quasi-phase matching (QPM), silicon-on-insulator (SOI), wavelength conversion.

1. Introduction

Recently, the silicon-on-insulator (SOI) waveguide has emerged as an attractive optical device due to its potential means to alleviate the urgent demands on electronics in the future optical communications. Because of good optical field confinement and large nonlinear coefficient, the SOI waveguide-based planar devices can be integrated with the state of art integrated circuits.

Recently, lots of studies have concentrated on studying the nonlinear optical phenomena in SOI waveguide. Significant works, including the Raman laser [1], [2], parametric amplification [3], [4], wavelength conversion [5]–[8], and the all optical switch [9], [10] have been reported. Four-wave mixing (FWM) based broadband parametric wavelength conversion in SOI waveguide has attracted considerable interests because it can realize the parallelism of information transferring and processing in the multiple wavelength channels [5], [6]. However, FWM as a parametric process is very sensitive to the relative phase-mismatch between the pump, signal, and idler, which can cause the periodical power fluctuation of the idler. Thus, the main challenge to realize broadband FWM-based wavelength conversion is to optimize the phase-matched condition induced by dispersion and nonlinearity effects.

The waves involved in FWM process can be phase-matched through pumping near the zero dispersion wavelength (ZDWL) of SOI waveguide [6], [8], but it requires the careful design of the waveguide geometry so as to reduce the phase-mismatch. Recently, the quasi-phase matching (QPM) technique was proposed to periodically reset the phase-mismatch [11]. This technique could realize efficient wavelength conversion in the case of serious phase-mismatch, which provides more freedom to design the waveguide geometry. However, it is difficult to realize the QPM on SOI platform due to large Kerr coefficient and strong nonlinear loss induced by two-photon absorption (TPA) and free carrier absorption (FCA) [12], [13]. Although some schemes were proposed to solve the problem, the conversion efficiency was only enhanced at the designed wavelength [12]–[14]. As reported in our previous work, the single-period vertical grating can be used for extending the conversion bandwidth by alternating the phase-mismatch between two values with opposite signs, but the QPM scheme in single-period grating waveguide (SPG-w) suffers from the strong nonlinear absorption [15].

Here, a novel SOI waveguide with the multi-period silicon grating is presented. The multi-period grating waveguide (MPG-w) is utilized to strictly limit the phase-mismatch to a small range in the former part of SOI waveguide. Compared with the SPG-w, the numerical results show that both the conversion efficiency and 3-dB bandwidth can be efficiently enhanced. It is possible to simplify the waveguide structure when the optimal parameters are chosen.

2. Principle

During the FWM process, the powers of pump P_p, signal P_s, and idler P_i in silicon waveguide can be described by the following equations that take into account of TPA, FCA, free carrier dispersion (FCD), and Kerr effects [15], [16]:

$$\frac{dP_p}{dz} = -\left[\frac{c\kappa_p^N}{nv_{g,p}}\left(\alpha+\alpha_p^{\mathrm{FCA}}\right)+2\beta_p^{\mathrm{TPA}}P_p\right]P_p - 4Re(\Gamma_{pspi})\left(P_p^2P_sP_i\right)^{\frac{1}{2}}\sin\theta \tag{1}$$

$$\frac{dP_{k=s,i}}{dz} = -\left[\frac{c\kappa_k^N}{nv_{g,k}}\left(\alpha+\alpha_k^{\mathrm{FCA}}\right)+2\beta_{kp}^{\mathrm{TPA}}P_p\right]P_k + 2Re(\Gamma_{kplp})\left(P_p^2P_sP_i\right)^{\frac{1}{2}}\sin\theta \tag{2}$$

$$\frac{d\theta}{dz} = \kappa + Re\left[\Gamma_{spip}\left(P_p^2P_i/P\right)_s^{\frac{1}{2}}+\Gamma_{ipsp}\left(P_p^2P_s/P\right)_i^{\frac{1}{2}}-4\Gamma_{pspi}(P_sP_i)^{\frac{1}{2}}\right]\cos\theta \tag{3}$$

$$\kappa = \Delta\beta + 2\,Re(\Gamma_{sp}+\Gamma_{ip}-\Gamma_p)P_p - \kappa_{\mathrm{FCD}} \tag{4}$$

where α and $v_{g,j}$ represent the linear loss and group velocity, respectively. Here, κ_j^{N} is the confinement factor that corresponds to the power scale of the wave j confined within the silicon. The coefficient $\alpha_j^{\mathrm{FCA}} = 1.45\times10^{-17}(\lambda_j/\lambda_{\mathrm{ref}})^2N$ and $\delta n_j^{\mathrm{FC}} = (-8.8\times10^{-4}N - 8.5N^{0.8})\times10^{-18}$ describe the absorption and index change of free carriers, respectively. The reference wavelength λ_{ref} is located at 1550 nm. $N = \tau_0\beta_{\mathrm{TPA}}|A_p|^4/2\hbar\omega_p a_p^2$ represents the density of free carriers generated by TPA, $\tau_{\mathrm{o}} = 1$ ns is the lifetime of the free carrier, and α_p is the effective modal area of

the pump. N and α_j^{FCA} have units of cm^{-3} and cm^{-1}. The parameter Γ_{klmn} is defined as [14], [15], [17]

$$\Gamma_{klmn} = \frac{3\omega_k \eta_{klmn}}{4\varepsilon_0 c^2 \bar{a} (n_k n_l n_m n_n)^{\frac{1}{2}}} \chi^{(3)}_{klmn} = \frac{n_2 \omega_k \eta_{klmn}}{c\bar{a}} + i\frac{\beta_{\mathrm{TPA}} \eta_{klmn}}{2\bar{a}} \tag{5}$$

The indices k, l, m, and n refer to p, s, and i in Eq. (1)–(3), $n_{\mathrm{v}}(\omega_{\mathrm{v}})$ $(v = i, j, k, l)$ is the modal refractive index at ω_v, and $\bar{a}$ is the average effective mode area given by $\bar{a} = (a_k a_l a_m a_n)$. Here $\chi^{3)}_{klmn}$ is the third-order susceptibility tensor. The Kerr coefficient n_2 and the TPA coefficient β_{TPA} are related to the real and imaginary part of the tensor. Based on the measurements carried out to characterize n_2 and β_{TPA} over a wide frequency range [18]–[24], the value of n_2 for silicon is 6×10^{-5} cm^2/W, and the β_{TPA} is 0.45 cm/GW at near-infrared wavelength. $\eta_{klmn} = \iint F_k^* F_l F_m^* F_n dA / (\Pi_{v=k,l,m,n} \iint |F_v|^2 dA)^{1/4}$ is the mode-overlap factor [16], where F_v is the mode profile transverse to the propagating direction. Equation (4) includes the wavelength-dependent parameters, such as nonlinear parameters, mode-overlap factor, and modal refractive index. When only one wave at ω_{i} is propagated, $\eta_{\mathrm{iiii}} = 1$, and (5) is reduced to the conventional nonlinear parameter [16], [25]. The waves in (1)–(3) are assumed to be the fundamental TE mode so that the Raman scattering could be neglected [8], [12]–[15], [26].

Here $\theta(z) = \Delta\beta z + \phi_s(z) + \phi_i(z) - 2\phi_p(z)$ is phase-mismatch of the co-propagating waves, $k = s$, i holds when $l = i$, s. κ is the phase-mismatch and κ_{FCD} induced by FCD can be neglected at low pump power [4], [16]. Equations (1) and (2) describe the power conversion rate in the waveguide, indicating that θ determining the directions of power flow in FWM process. If $\sin\theta > 0$, $dP_{\mathrm{p}}/dz < 0$ in (1), indicating the power being converted from the pump to signal and idler. If $\sin\theta < 0$, $dP_k/dz < 0$ in (2), indicating that the power being converted from the signal and idler to the pump. For a constant-width waveguide (CW-w), the power of idler becomes fluctuation due to the large phase-mismatch. When a QPM scheme is utilized, the phase-mismatch is periodically reset between two values with the opposite signs, and the phase-mismatch can be controlled to ensure that $\sin\theta > 0$ along the waveguide. The power back conversion is suppressed, and a higher conversion efficiency is achieved. It is evident that the factor $\mathrm{Re}(\Gamma_{klmn})(P_p P_s P_i)^{1/2}\sin\theta$ in (1) and (2) determines the conversion rate of power. The traditional QPM would keep the conversion rate $dP_k/dz > 0$ all along the waveguide. However, due to the nonlinear absorptions, the linear attenuation and energy transfer, the pump power P_{p} along the silicon waveguide is dramatically reduced, which induces a significantly decrease of the factor $\mathrm{Re}(\Gamma_{klmn})(P_p P_s P_i)^{1/2}\sin\theta$ during the propagation. The decrease of factor makes the QPM in silicon waveguide more difficult since the first term in (2), which represents the linear loss and nonlinear absorptions, is quite large and negative. The large Kerr coefficient also make the decrease of the factor more obvious. During the propagation, the power of pump in the former part of the waveguide is larger than the back part due to the large loss and nonlinear absorption of silicon waveguide. The QPM is more sensitive to the phase-mismatch in the former part. By changing the structure of the former part of the waveguide, the phase-mismatch is restricted to a small value, and the power of idler can be enhanced. (4) shows the total phase-mismatch κ. Here the first part $\Delta\beta$ is the linear phase-mismatch between the pump, signal, and idler. Other parts are induced by the nonlinearities such as nonlinear absorption and FWM process. Only the linear phase-mismatch can be directly controlled by changing the cross-section of waveguide [14], [27], [28]. The linear phase-mismatch $\Delta\beta$ is determined by the second-order dispersion $\beta_{2,\mathrm{p}}$ and fourth-order dispersion $\beta_{4,\mathrm{p}}$ [5]:

$$\Delta\beta \approx -\beta_{2,p}(\omega_p - \omega_s)^2 - \frac{\beta_{4,p}}{12}(\omega_p - \omega_s)^4. \tag{6}$$

In our investigation, the QPM scheme is achieved by using the rectangular SOI waveguide with air cladding, as shown in Fig. 1(a). The waveguide height h is set to be 220 nm. The

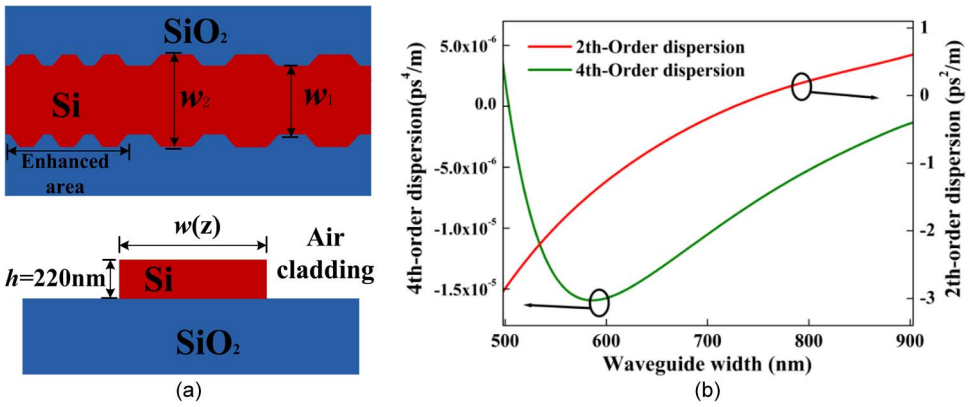

Fig. 1. (a) Conceptual illustration of the MPG-w, and (b) second-order and fourth-order dispersion at 1550 nm as a function of the waveguide width.

second-order and fourth-order dispersions $\beta_{2,p}$ and $\beta_{4,p}$ at 1550 nm as a function of w are shown in Fig. 1(b). It can be seen the phase-mismatch can be periodically reset between two values with opposite signs by changing the waveguide width which creates the waveguide grating. So even the phase-mismatch is serious, which corresponds to a larger $\Delta\beta$, the mismatch phase θ will be controlled within a smaller range with $\theta \propto \Delta\beta_+ L_1 + \Delta\beta_- L_2$ inferred from (4). Here $\Delta\beta_{+(-)}$ means the phase-mismatch between the co-waves, the indices "+" and "−" means the sign of $\Delta\beta$. L_1 and L_2 are the lengths of grating that correspond to the waveguide width w_1 and w_2, respectively. In the MPG-w the grating length $L_{1,2}$ is reduced in the enhanced area, where the range of phase-mismatch is also decreased. The structure of the proposed waveguide is shown in Fig. 1(a), where the waveguide width is set to be w_1 and w_2 periodically and the period of gratings in the enhancing area is smaller. It is evident that the effective area is also changed by the waveguide width, and both of the nonlinear coefficient Γ and linear phase-mismatch are periodically changed along the waveguide.

The QPM scheme in the MPG-w is described as

$$\Delta\beta_{sw}(z) = \begin{cases} \Delta\beta_+ & \text{if } w = w_1 \\ \Delta\beta_- & \text{if } w = w_2 \end{cases} \tag{7}$$

where $\Delta\beta_{sw}$ is the linear phase-mismatch between λ_s and λ_p in SOI waveguide. When $\theta(0) = \pi/2$, the phase-mismatch factor $\Delta\beta_+$ and $\Delta\beta_-$ have the relations:

$$\Delta\beta_+ L_{f,1} = -\Delta\beta_- L_{f,2} = \frac{\pi}{2} \tag{8}$$

$$\Delta\beta_+ L_{b,1} = -\Delta\beta_- L_{b,2} = \pi \tag{9}$$

where $L_{f(b),1}$ and $L_{f(b),2}$ are the length of gratings corresponding to the waveguide width w_1 and w_2. The periods of grating in the enhanced area Λ_{enha} and back part Λ_{back} are $\Lambda_{enha} = L_{f,1} + L_{f.2}$ and $\Lambda_{back} = L_{b,1} + L_{b,2}$, respectively. The indices f and b mean the former and back part of the waveguide. In the previous works [14], [15], the QPM scheme is induced by the single-period grating, as described by (9). In the MPG-w, Equations (8) and (9) indicate that the range of phase θ is within $\pi/2$ in the former part, and changed to π in the back part. The values of $\sin\theta$ in (1) and (2) are close to 1 in the enhanced area, which contributes a larger rate of power conversion compared to the SPG-w.

In addition, the variation of w will induce the mode mismatch and the additional back reflection loss. Hence a linear taper is utilized to connect w_1 and w_2 to reduce the loss [14], [29]–[31]. The waveguide width is changed linearly from w_1 (or w_2) to w_2 (or w_1), as shown in Fig. 1(a). Equation (8) indicates that the length of grating $|\Delta\beta|L_{grating}$ should equal to $\pi/2$. Based on the analysis in [14], the taper length should have a limitation of $|\Delta\beta|L_{taper} < \pi/2$. Here, we set

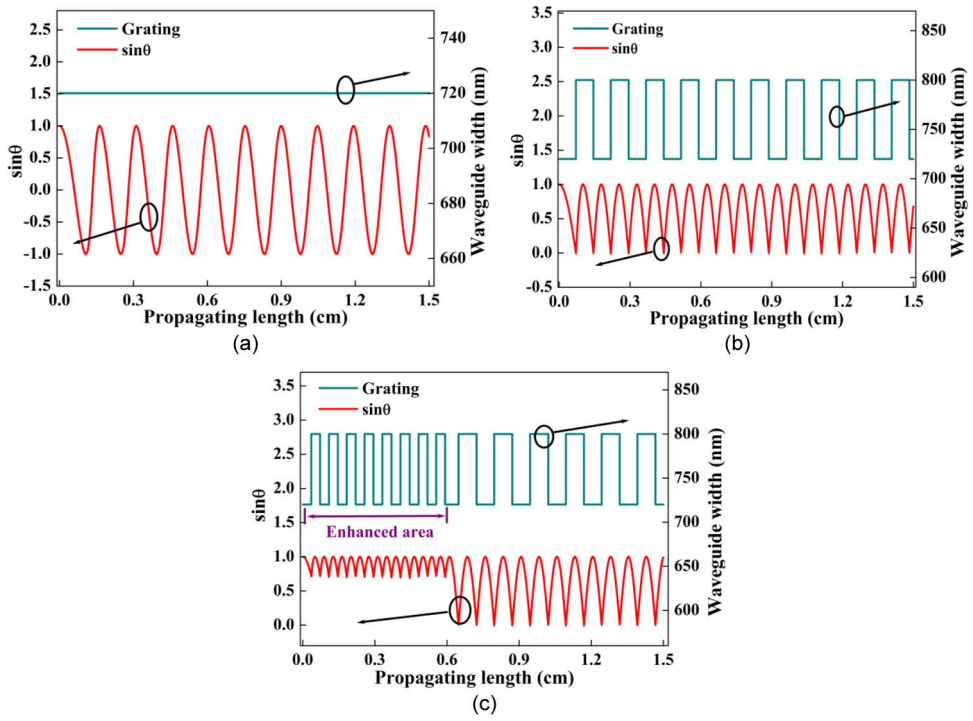

Fig. 2. Waveguide width of (a) the CW-w, (b) SPG-w, and (c) MPG-w and the value of $\sin\theta$ as a function of propagating length.

$L_{\text{taper}} = 25\ \mu$m as in [14], it can be inferred that the linear phase-mismatch $|\Delta\beta$ should be less than 628.3/cm. Such a value is translated to be $|\beta_{2,\text{p}}| < 3.2\ \text{ps}^2/\text{m}$ when the wavelengths of pump and signal are chosen as 1550 and 1750 nm. As seen from Fig. 1(b), it is evident that such a value will not limit the width of waveguide since the value of 3.2 ps^2/m is much larger than $\beta_{2,\text{p}}$ in Fig. 1(b).

3. Simulation Results and Discussions

In the simulation, the pump at $\lambda_{\text{p}} = 1550$ nm and signal at $\lambda_{\text{s}} = 1750$ nm are used. The powers of the pump and signal are 250 mW and 120 μW, respectively. The linear loss coefficient is 1.5 dB/cm for $w_1 = 720$ nm and $w_2 = 800$ nm. Note that the waveguide width shift is 80 nm and the taper length is 25 μm, which is nearly the order of 3 larger than the width shift. Such a length of taper can efficiently reduce the back reflection loss [14], [29]–[31]. The value of $\sin\theta$ as a function of propagating length is shown in Fig. 2. As shown in Fig. 2(a), the $\sin\theta$ is changed from -1 to $+1$ in the SOI waveguide with constant width $w = 720$ nm. This is induced by the large phase-mismatch between the pump $\lambda_{\text{p}} = 1550$ nm, signal $\lambda_{\text{s}} = 1750$ nm, and idler $\lambda_{\text{i}} = 1391$ nm. Fig. 2(b) shows the waveguide with the single-period grating. When $\sin\theta = 0$, a phase shift of π is induced by changing the waveguide width, and $\sin\theta$ is positive along the waveguide. The multi-period grating is illustrated in Fig. 2(c). The value of $\sin\theta$ is close to 1 in the enhanced area. The length of enhanced area is 0.6 cm, which is suitable for the tradeoff between grating number and conversion effects.

The conversion efficiency as a function of propagation length is shown in Fig. 3, which is given by $\eta_c = 10\log[P_{\text{idler}}(L)/P_{\text{signal}}(0)]$. Here L, $P_{\text{idler}}(L)$, and $P_{\text{signal}}(0)$ represent the length of waveguide, the output idler power, and the input signal power, respectively. Fig. 3(a) shows the conversion efficiency at $\lambda_{\text{s}} = 1750$ nm as a function of propagating length. It is evident that the CW-w induces the power fluctuation due to the large phase-mismatch, and the final conversion efficiency of -40.8 dB is achieved. The SPG-w suppresses the power fluctuation along the

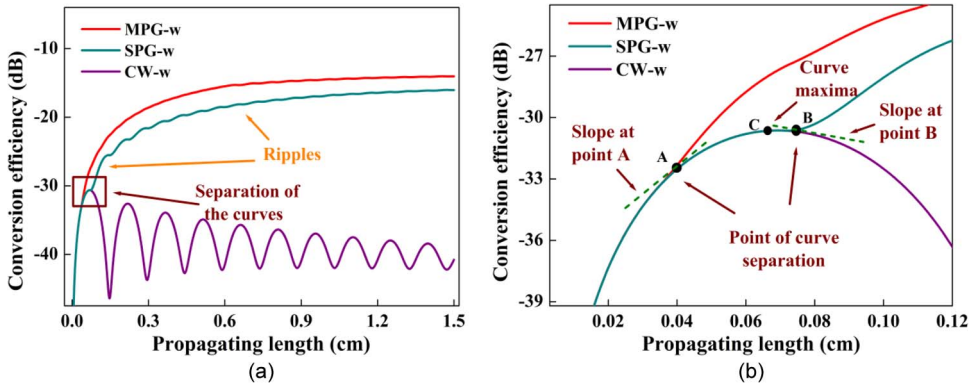

Fig. 3. (a) Conversion efficiency as a function of propagating length in CW-w, SPG-w, and MPG-w, and (b) the magnified picture of separate region in (a).

waveguide, and the conversion efficiency is increased to -16.1 dB. It is evident that the power of idler in MPG-w increases faster than the others since the value of $\sin\theta$ is close to 1 in the enhanced area. The corresponding power conversion rate dP_i/dz is larger, and the higher conversion efficiency is obtained in MPG-w. The conversion efficiency in the MPG-w can be up to -14.0 dB, achieving an enhancement of 26.8 dB compared with CW-w and an increase of 2.1 dB compared with SPG-w. In addition, the proposed waveguide shows a higher conversion efficiency when compared with the similar works in [14] and [15], where the conversion efficiency of -23 dB and -17 dB are obtained at 1750 nm with 300 mW pump at 1550 nm, respectively. The parameters such as the linear loss, Kerr coefficient, and lifetime of the free carrier are nearly the same. Hence it is convincing to show the better performance of the proposed waveguide since it enhances the conversion efficiency by using a lower pump power of 250 mW. To further clarify the effect of these gratings, the curves separate region is shown in Fig. 3(b). The curves of CW-w and SPG-w separate at point B. This point corresponds to $\sin\theta = 0$ because a phase shift of π is induced by changing waveguide width in SPG-w after point B. The curve of MPG-w is separated from SPG-w at point A. It can be noted that point A is before the curve maxima point C, and the point B is after the curve maxima. The slop at point A and B is positive and negative, respectively. In SPG-w, the $\sin\theta$ equals to zero at point B, and dP_i/dz equals to the first term in (2). Hence, the power conversion rate $dP_i/dz < 0$, the slope of point B is negative. For this reason, the power of idler wave is decreased when $\sin\theta$ is near the zero. During the propagation, $\sin\theta$ is changed from 1 to 0 periodically in SPG-w. When the value of $\sin\theta$ is quite close to zero, the first term in (2) makes the conversion rate $dP_i/dz < 0$. As the value of $\sin\theta$ is increased, the conversion rate is changed to be $dP_i/dz > 0$. This periodical change of conversion rate induces a ripple of the conversion efficiency curve in SPG-w, as illustrated in Fig. 3(a), and the ripple becomes smaller when propagating in the back part which indicates the conversion efficiency is more sensitive to the phase-mismatch in the former part of the waveguide. The ripple induces a slower increase of the idler power, which indicates that the power conversion suffers from the large loss and Kerr coefficient of SOI waveguide with the single-period grating. In contrast, the MPG-w makes the value of $\sin\theta$ close to 1 in the enhanced area. The second term at the right side in (2) makes the conversion rate $dP_i/dz > 0$ along the waveguide, which makes the slope at point A to be positive. Thus, the multi-period grating can circumvent the hurdle induced by the large loss of waveguide, and there is no obvious ripple as shown in Fig. 3(a), which can enhance the power conversion.

The conversion efficiency of different SOI waveguide is shown in Fig. 4. For the 720 nm CW-w, the 3-dB bandwidth is 89 nm. Another waveguide has the constant width of 755 nm which corresponds to the dispersion engineering waveguide (DE-w). It shows that the 3-dB bandwidth is increased to 304 nm by pumping near the ZDWL, and a broadband wavelength conversion is achieved. The QPM-gratings can make a further bandwidth enhancement. The

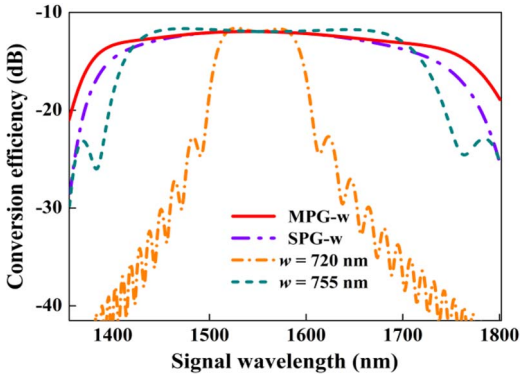

Fig. 4. Conversion efficiency spectra of different SOI waveguides.

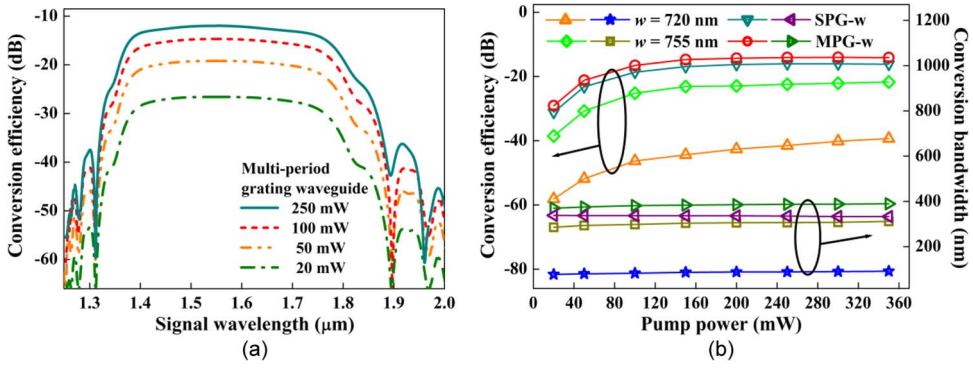

Fig. 5. (a) Dependence of conversion efficiency on the pump power in MPG-w and (b) conversion effects in different waveguides as a function of the pump power.

SPG-w realizes the bandwidth of 334 nm, which is 245 nm larger than that in the CW-w and 30 nm larger than that in the DE-w. The MPG-w performs a bandwidth of 387 nm, which is 53 nm larger than that of SPG-w. Compared with other works [14], [15], the bandwidth is still significantly increased. In [14] the bandwidth is quite small because it only converts the optics at the designed wavelength around 1750 nm. In [15], the SPG-w is used that realize a 331 nm bandwidth which is still smaller than our work. It can be noted that the conversion efficiency of the DE-w shows better when the signal is launched in the wavelength range of 1428 to 1699 nm. This is induced by the relatively smaller phase-mismatch in the FWM process since the wavelength of signal is not quite far from the pump. It is evident that the QPM gratings realize a higher conversion efficiency as the wavelength distance $\Delta\lambda_{s,p} = |\lambda_p - \lambda_s|$ is increased, which corresponds to the serious phase-mismatch. Especially when the signal is launched near 1350 or 1800 nm, an improvement of $\sim$6 dB is realized in the MPG-w compared with the SPG-w and DE-w.

The dependence of conversion efficiency on the pump power in MPG-w is shown in Fig. 5(a). As the power is increased, the higher conversion efficiency can be obtained. When the pump is stronger, the increment of pump contributes less to the conversion efficiency due to the large nonlinear absorptions induced by TPA and FCA. The conversion effects in different waveguides as a function of the pump power are shown in Fig. 5(b). The pump power has less influence on the conversion bandwidth, and the MPG-w contributes to the largest bandwidth. The conversion efficiency becomes saturate when the pump power reaches 200 mW due to the nonlinear losses. For the waveguide with $w = 720$ nm, the conversion efficiency is -39.3 dB when the pump is 350 mW, and a much higher value of -29.1 dB can be acquired with only 20 mW in MPG-w. Similarly, the saturate conversion efficiency of -14 dB is obtained with 250 mW in

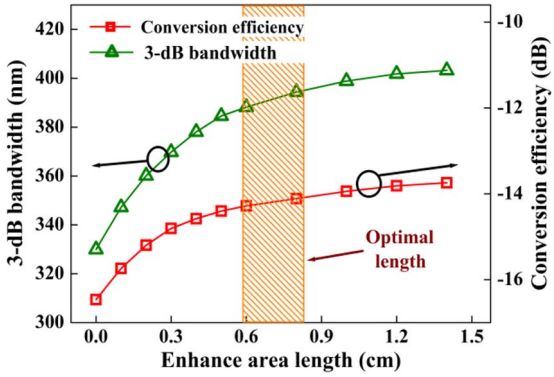

Fig. 6. Conversion efficiency of $\lambda_s = 1750$ nm and the 3-dB bandwidth as a function of the enhancing area length.

TABLE 1

Conversion effects in different SOI waveguides

Waveguide width (nm)	Phase-mismatch range	Grating number	Conversion efficiency (dB)	3-dB bandwidth (nm)
w_1=720, w_2=800	$\pi/2$	28	-14.0	387
w_1=720, w_2=780	$\pi/2$	22	-14.1	391
w_1=720, w_2=760	$\pi/2$	16	-13.9	399
w_1=720, w_2=760	$\pi/5$	18	-13.4	410
w = 755	2π	—	-22.1	304

SPG-w while the same value is acquired with 100 mW in MPG-w. For the CW pump, such a decrease on the pump power can improve the feasibility and save the energy of the device significantly.

The enhanced area is located in the former part of the SOI waveguide. As the length of enhanced area is increased, both of the idler power and the 3-dB bandwidth can be improved. However, the grating period in the enhanced area is smaller than that in the back part. Longer enhanced area means a larger number of gratings, which will increase the reflection loss and the fabrication difficulty. Fig. 6 shows the relationships between the conversion efficiency and the 3-dB bandwidth and the length of enhanced area. Both of the conversion efficiency and 3-dB bandwidth are increased with the increase of enhanced area length. Moreover, the improvement of conversion effects is not linear with the length of enhanced area, and tends to be saturated when the length reaches 0.6 to 0.8 cm. A longer length of enhanced area will no longer induces an efficient enhancement of the conversion effects.

Above all, the MPG-w significantly enhances the conversion effects over a broadband wavelength range. It can be seen from Fig. 1(b) and (6)–(9) that the smaller dispersion makes the phase change much slower with the propagating length. Hence the optimal value of w_2 in the enhanced area can simplify the structure of MPG-w by reducing the grating number. Furthermore, for the same grating number, the range of phase-mismatch in (8) can be set smaller than $\pi/2$ when the width of w_2 is optimized which can further enhance the conversion effects. Table 1 shows the 3-dB bandwidth and the conversion efficiency of signal at 1750 nm of different grating widths. The grating number is defined by $N_{\text{grating}} = 2(\Lambda_{\text{enha}} + \Lambda_{\text{back}})$, and the enhanced area is about 0.6 cm. It is evident that the grating number is smaller for the same phase-mismatch range when the width of w_2 is decreased. When w_2 is 760 nm, the period number is 16, which is even

smaller than that of SPG-w. It also shows that the conversion effects reach to -13.4 dB and 410 nm for a smaller phase-mismatch range of $\pi/5$. Hence the proposed waveguide has the potential to realize the enhancement of conversion effects over a broad wavelength range. Compared with the 755 nm DE-w, the MPG-w performs a better conversion effects, and contributes to the enhancement of $\sim$8 dB and $\sim$100 nm of conversion effects. And it shows that different structures of the MPG-w can be chosen to realize the broadband enhancement of conversion effects which brings more freedom of the waveguide design.

4. Conclusion

In summary, a SOI waveguide with the multi-period vertical grating is proposed. The grating realizes the QPM scheme in FWM process by overcoming the difficulty caused by the large Kerr coefficient and nonlinear absorptions and contributes to a better conversion effects even if the phase-mismatch of co-waves are serious. It is found that the conversion efficiency and the 3-dB conversion bandwidth at designated signal wavelength can be enhanced evidently in the proposed waveguide without dispersion engineering. By optimizing the length of enhanced area and the width of grating, a wavelength conversion with the efficiency of -13.4 dB and the bandwidth of 410 nm can be achieved when the phase-mismatch w_1 and w_2 are $\pi/5$, 720, and 760 nm, respectively. The study results show that the proposed SOI waveguide is an ideal device for the broadband wavelength conversion.

References

[1] F. De Leonardis, B. Troia, and V. M. N. Passaro, "Design rules for Raman lasers based on SOI racetrack resonators," *IEEE Photon. J.*, vol. 5, no. 6, Dec. 2013, Art. ID. 1502431.
[2] H. Rong *et al.*, "A continuous Raman silicon laser," *Nature*, vol. 433, no. 7027, pp. 725–728, Feb. 2005.
[3] M. A. Foster *et al.*, "Broad-band optical parametric gain on a silicon photonic chip," *Nature*, vol. 441, no. 7096, pp. 960–963, Jun. 2006.
[4] X. Sang and O. Boyraz, "Gain and noise characteristics of high-bit-rate silicon parametric amplifiers," *Opt. Exp.*, vol. vol. 16, no. 17, pp. 13 122–13 132, Aug. 2008.
[5] M. A. Foster, A. C. Turner, R. Salem, M. Lipson, and A. L. Gaeta, "Broad-band continuous-wave parametric wavelength conversion in silicon nanowaveguides," *Opt. Exp.*, vol. 15, no. 20, pp. 12 949–12 958, Oct. 2007.
[6] A. C. Turner-Foster, M. A. Foster, R. Salem, A. L. Gaeta, and M. Lipson, "Frequency conversion over two-thirds of an octave in silicon nanowaveguides," *Opt. Exp.*, vol. 18, no. 3, pp. 1904–1908, Feb. 2010.
[7] Y. Okawachi, A. L. Gaeta, and M. Lipson, "Breakthroughs in nonlinear silicon photonics 2011," *IEEE Photon. J.*, vol. 4, no. 2, pp. 600–606, Apr. 2012.
[8] Q. Lin, J. Zhang, P. M. Fauchet, and G. P. Agrawal, "Ultrabroadband parametric generation and wavelength conversion in silicon waveguides," *Opt. Exp.*, vol. 14, no. 11, pp. 4786–4799, May 2006.
[9] O. Boyraz, P. Koonath, V. Raghunathan, and B. Jalali, "All optical switching and continuum generation in silicon waveguides," *Opt. Exp.*, vol. vol. 12, no. 17, pp. 4094–4102, Aug. 2004.
[10] V. R. Almeida *et al.*, "All-optical switching on a silicon chip," *Opt. Lett.*, vol. 29, no. 24, pp. 2867–2869, Dec. 2005.
[11] J. Kim, O. Boyraz, J. H. Lim, and M. N. Islam, "Gain enhancement in cascaded fiber parametric amplifier with quasi-phase matching: Theory and experiment," *J. Lightw. Technol.*, vol. 19, no. 2, pp. 247–251, Feb. 2001.
[12] J. B. Driscoll *et al.*, "Directionally anisotropic Si nanowires: On-chip nonlinear grating devices in uniform waveguides," *Opt. Lett.*, vol. 36, no. 8, pp. 1416–1418, Apr. 2011.
[13] J. B. Driscoll *et al.*, "Width-modulation of Si photonic wires for quasi-phase-matching of four-wave-mixing: Experimental and theoretical demonstration," *Opt. Exp.*, vol. 20, no. 8, pp. 9227–9242, Apr. 2012.
[14] Y. Lefevre, N. Vermeulen, and H. Thienpont, "Quasi-phase-matching of four-wave-mixing-based wavelength conversion by phase-mismatch switching," *J. Lightw. Technol.*, vol. 31, no. 13, pp. 2113–2121, Jul. 2013.
[15] B. Jin *et al.*, "Efficient and broadband parametric wavelength conversion in a vertically etched silicon grating without dispersion engineering," *Opt. Exp.*, vol. 22, no. 6, pp. 6257–6268, Mar. 2014.
[16] D. W. Kim *et al.*, "Enhanced four-wave-mixing effects by large group indices of one-dimensional silicon photonic crystal waveguides," *Opt. Exp.*, vol. 21, no. 24, pp. 30 019–30 029, Dec. 2013.
[17] Q. Lin,O. J. Painter, and G. P. Agrawal, "Nonlinear optical phenomena in silicon waveguides: Modeling and applications," *Opt. Exp.*, vol. 15, no. 25, pp. 16 604–16 644, Dec. 2007.
[18] M. Dinu, F. Quochi, and H. Garcia, "Third-order nonlinearities in silicon at telecom wavelengths," *Appl. Phys. Lett.*, vol. 82, no. 18, pp. 2954–2956, May 2003.
[19] R. Claps, D. Dimitropoulos, V. Raghunathan, Y. Han, and B. Jalali, "Observation of stimulated Raman amplification in silicon waveguides," *Opt. Exp.*, vol. 11, no. 15, pp. 1731–1739, Jul. 2003.
[20] H. K. Tsang *et al.*, "Optical dispersion, two-photon absorption, and self-phase modulation in silicon waveguides at 1.5 μm wavelength," *Appl. Phys. Lett.*, vol. 80, no. 3, pp. 416–418, Jan. 2002.
[21] G. W. Rieger, K. S. Virk, and J. F. Yong, "Nonlinear propagation of ultrafast 1.5 μm pulses in high-index-contrast silicon-on-insulator waveguides," *Appl. Phys. Lett.*, vol. 84, no. 6, pp. 900–902, Feb. 2004.

[22] V. Raghunathan, R. Shori, O. M. Stafsudd, and B. Jalali, "Nonlinear absorption in silicon and the prospects of mid-infrared silicon Raman lasers," *Phys. Stat. Sol. (A)*, vol. 203, no. 5, pp. R38–R40, Apr. 2006.
[23] A. D. Bristow, N. Rotenberg, and H. M. van Driel, "Two-photon absorption and Kerr coefficients of silicon for 850–2200 nm," *Appl. Phys. Lett.*, vol. 90, no. 19, May 2007, Art. ID. 191104.
[24] Q. Lin *et al.*, "Dispersion of silicon nonlinearities in the near-infrared region," *Appl. Phys. Lett.*, vol. 90, no. 2, Jul. 2007, Art. ID. 021111.
[25] G. P. Agrawal, *Nonlinear Fiber Optics*, 4th ed. Amsterdam, The Netherlands: Elsevier, 2007.
[26] I. D. Rukhlenko, M. Premaratne, and G. P. Agrawal, "Nonlinear silicon photonics: Analytical tools," *IEEE J. Sel. Topics Quantum Electron.*, vol. 16, no. 1, pp. 200–215, Jan./Feb. 2010.
[27] M. Zhu *et al.*, "Ultrabroadband flat dispersion tailoring of dual-slot silicon waveguides," *Opt. Exp.*, vol. 20, no. 14, pp. 15 899–15 907, Jul. 2012.
[28] A. C. Turner *et al.*, "Tailored anomalous group-velocity dispersion in silicon channel waveguides," *Opt. Exp.*, vol. 14, no. 10, pp. 4357–4362, May 2006.
[29] V. R. Almeida, R. R. Panepucci, and M. Lipson, "Nanotaper for compact mode conversion," *Opt. Lett.*, vol. 28, no. 15, pp. 1302–1304, Aug. 2003.
[30] M. L. Povinelli, S. G. Johnson, and J. D. Joannopoulos, "Slow-light, band-edge waveguides for tunable time delays," *Opt. Exp.*, vol. 13, no. 18, pp. 7145–7159, Sep. 2005.
[31] S. G. Johnson *et al.*, "Adiabatic theorem and continuous coupled-mode theory for efficient taper transitions in photonic crystals," *Phys. Rev. E, Stat. Nonlin. Soft Matter Phys.*, vol. 66, no. 6, Dec. 2002, Art. ID. 006608.